Physical Plasma Parameters Along The Full Loop Length of a Coronal Loop

Girjesh R. Gupta[1], Durgesh Tripathi[1], Helen Mason[2]

Inter-University Centre for Astronomy and Astrophysics (IUCAA), Pune, India
Department of Applied Mathematics and Theoretical Physics, University of Cambridge, UK
E-mail: girjesh@iucaa.ernet.in, durgesh@iucaa.ernet.in, h.e.mason@damtp.cam.ac.uk

Abstract: Coronal loops are the basic structures of the solar corona. Understanding of the physical mechanisms behind the loop heating, plasma flows, and filling are still considered a major challenge in solar physics. This problem makes coronal loops an interesting target for detailed study. We present spectroscopic observations of a full coronal loop in various spectral lines as recorded by the Extreme-ultraviolet Imaging Spectrometer on-board Hinode. We derive physical plasma parameters such as electron density, temperature, and filling factors along the loop length from one footpoint to the another. The obtained parameters indicate that loop has asymmetric density distribution with respect to gravitational stratification of the solar atmosphere. These new measurements of physical plasma parameters may provide important constraints on the modeling of the mass and energy balance in coronal loops.

Observations: A coronal loop from one footpoint to another was detected in an active region, AR 11131, observed on 2010 December 11 with EIS (Culhane et al. 2007) on board Hinode. Observations were carried out with the 2″ slit with an exposure time of 35 s, and a sparse raster of the region was created with a step size of 3″.

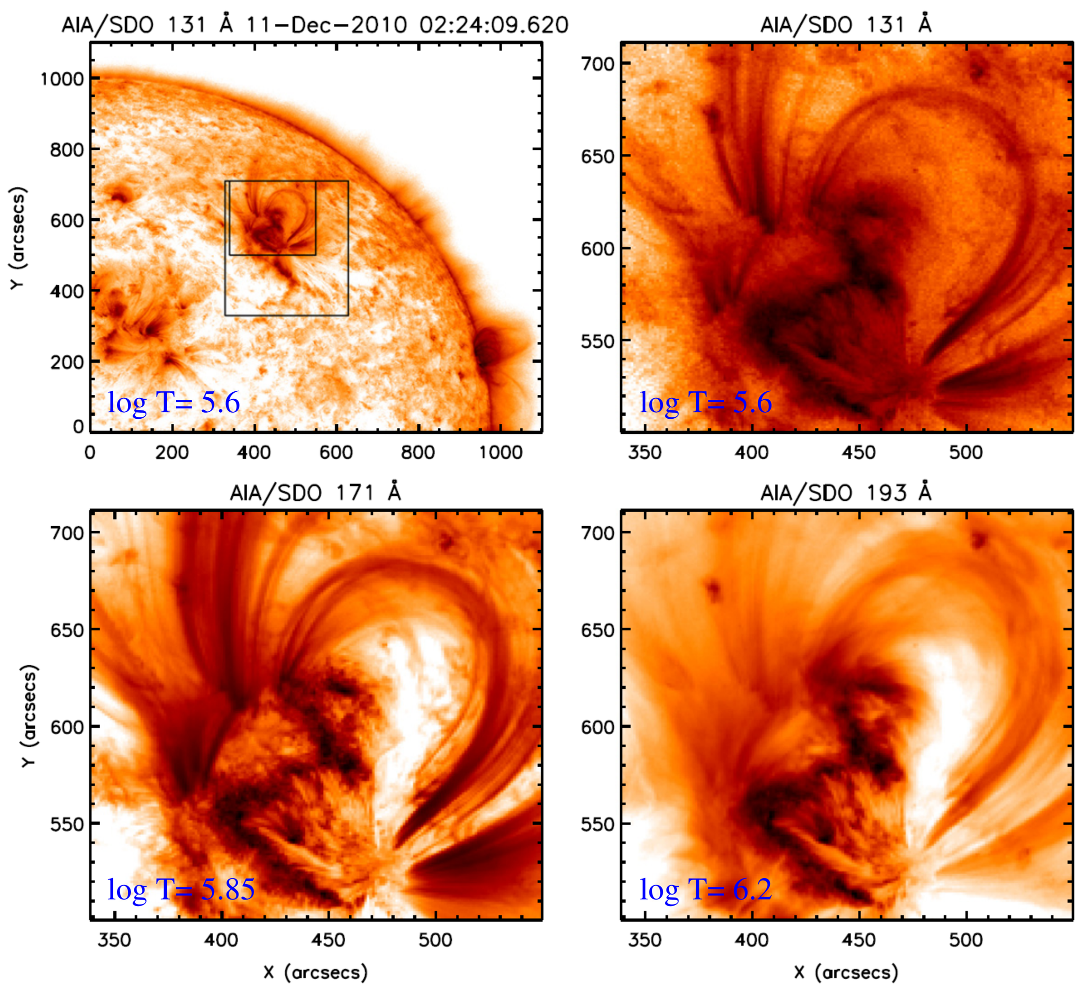

Figure 1. Top left image: a portion of the Sun's disk showing the active region AR 11131 in the 131 Å passband. The bigger box indicates the region rastered by EIS/Hinode. The smaller box is shown in subsequent images taken in the AIA 131 Å, 171 Å, and 193 Å passbands, as labeled.

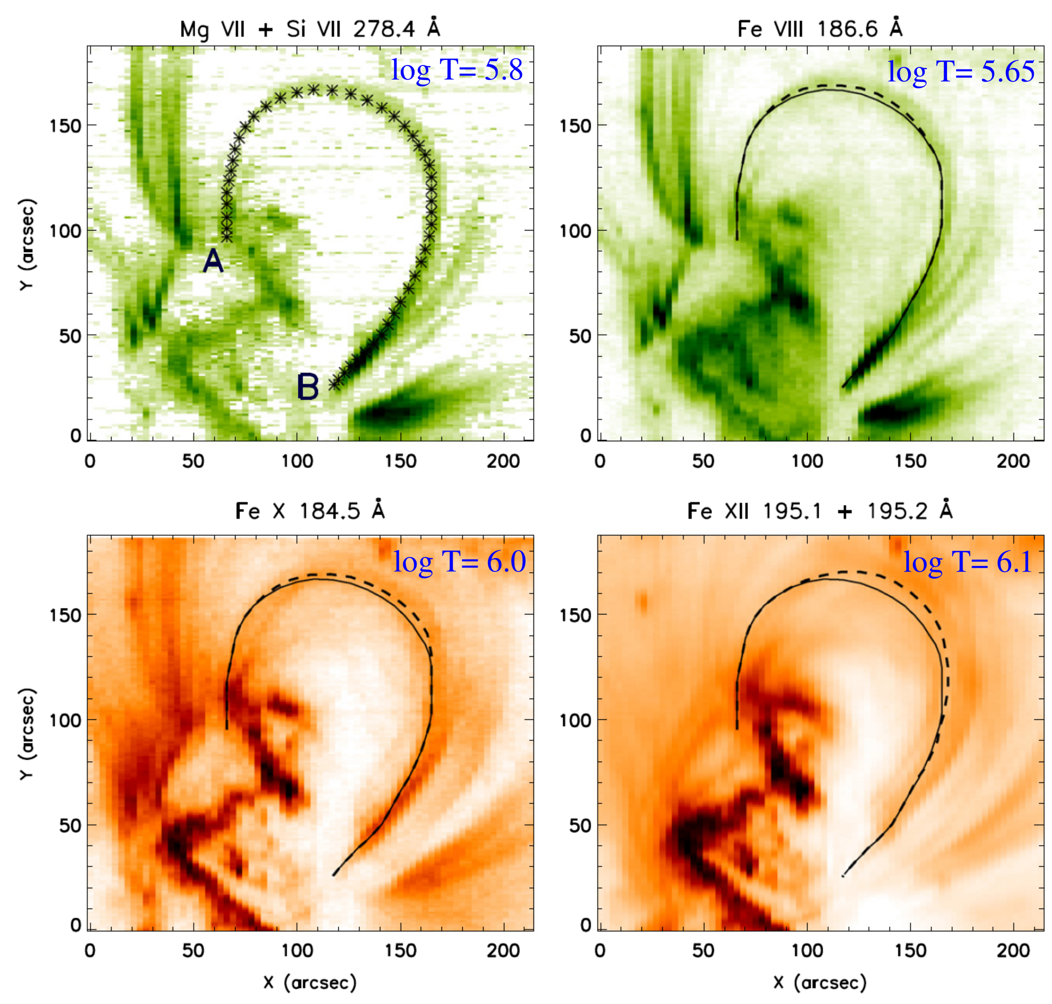

Figure 2. Traced coronal loop from left footpoint A to right footpoint B as seen in the Mg VII 278.39 Å (blended with Si VII 278.44 Å) spectral line (top left), Fe VIII 186.6 Å (top right), Fe X 184.5 Å (bottom left), and Fe XII 195.12 Å (blended with Fe XII 195.18 Å; bottom right). The traced loop structure from Mg VII 278.39 Å is also overplotted with a continuous line in all of the other panels.

Results:

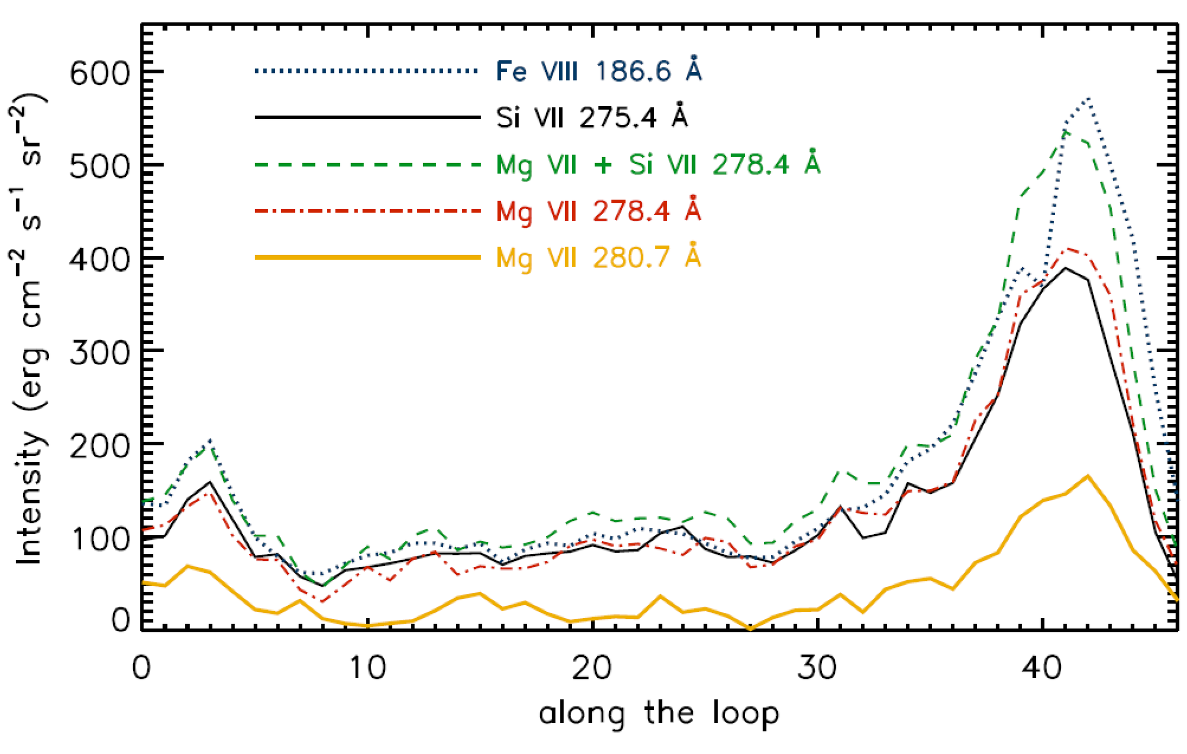

Figure 3. Variation in intensity along the coronal loop from footpoint A to B as measured in different spectral lines from EIS/Hinode.

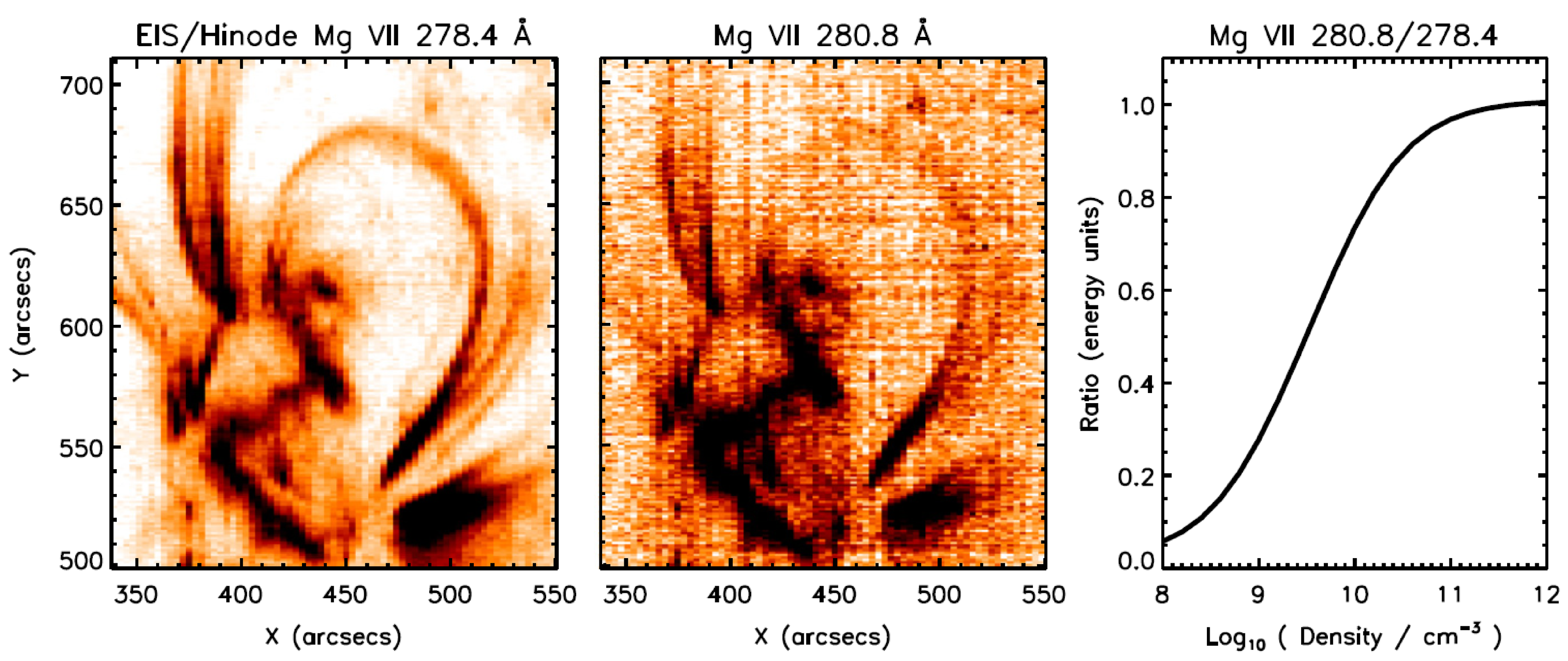

Figure 4. Intensity maps of the coronal loop obtained in the Mg VII 278.39 Å (left panel) and 280.75 Å (middle panel) spectral lines. The intensity ratio of the two spectral lines is sensitive to the electron density, and the variation is obtained from CHIANTI version 7.1 (right panel).

A) Density along the loop length:

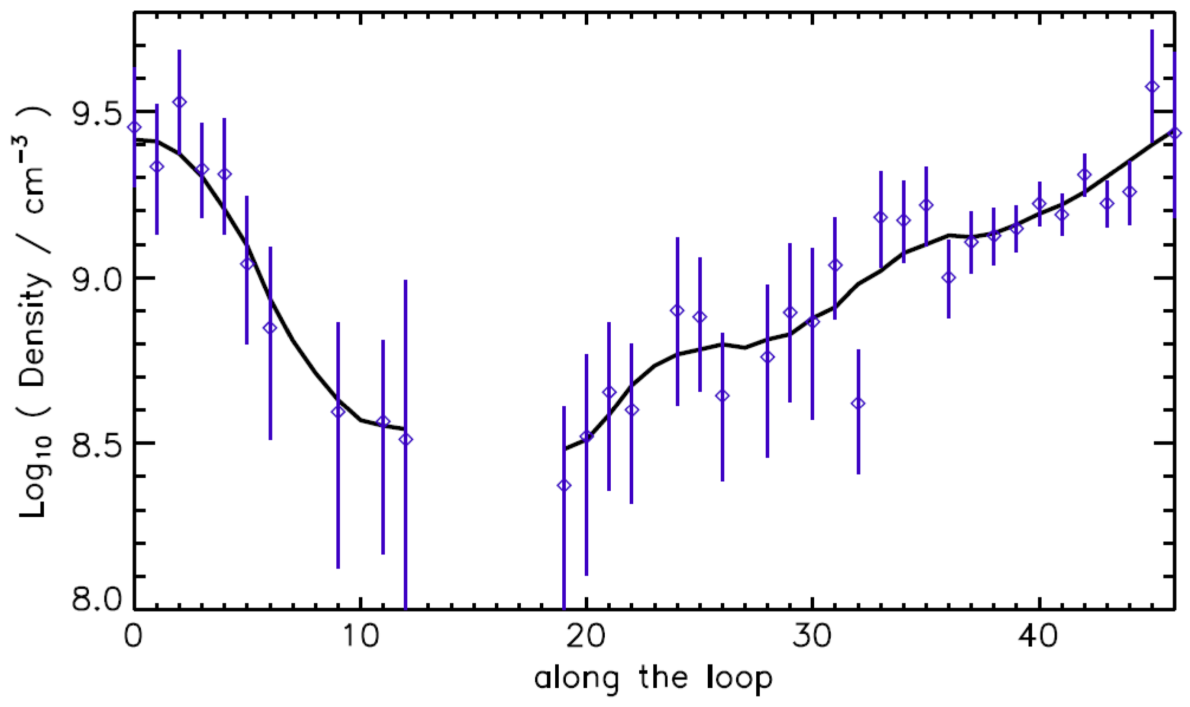

Figure 5. Density measured along the coronal loop from footpoint A to B using the Mg VII 280.75/278.39 line ratio.

B) Temperature along the loop length:

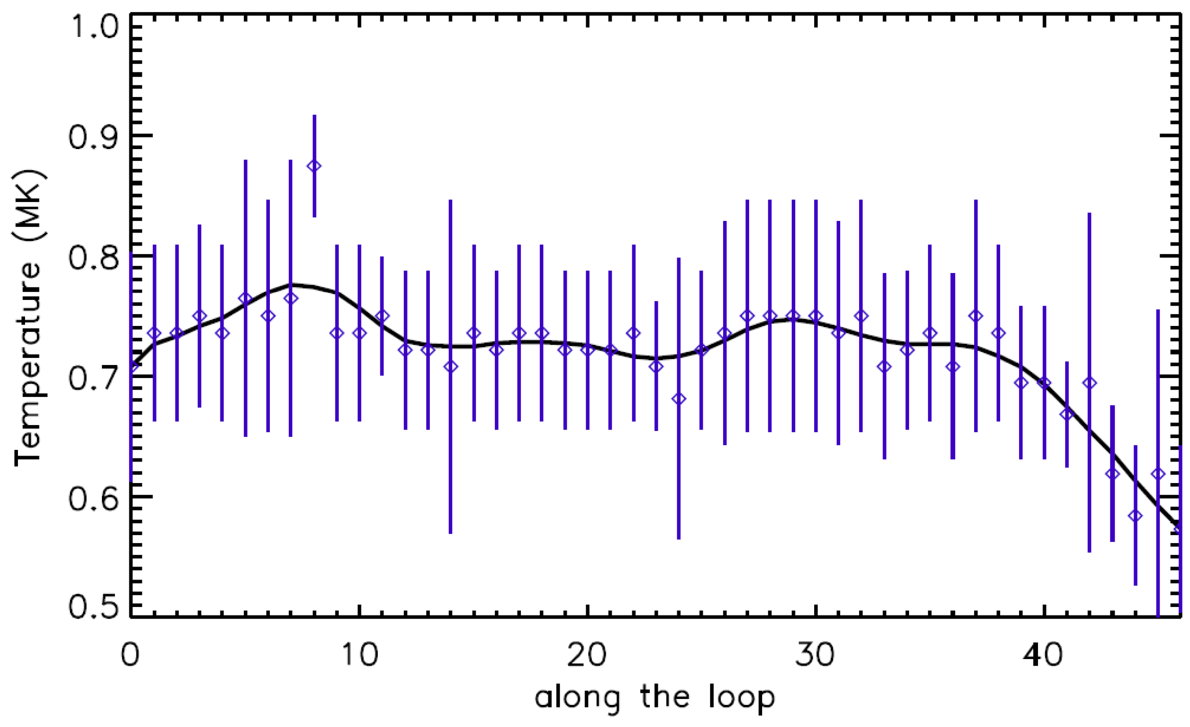

Figure 6. Temperature variation along the coronal loop footpoint A to B as obtained from the EM loci curves (not shown here).

C) Filling factor along the loop length:

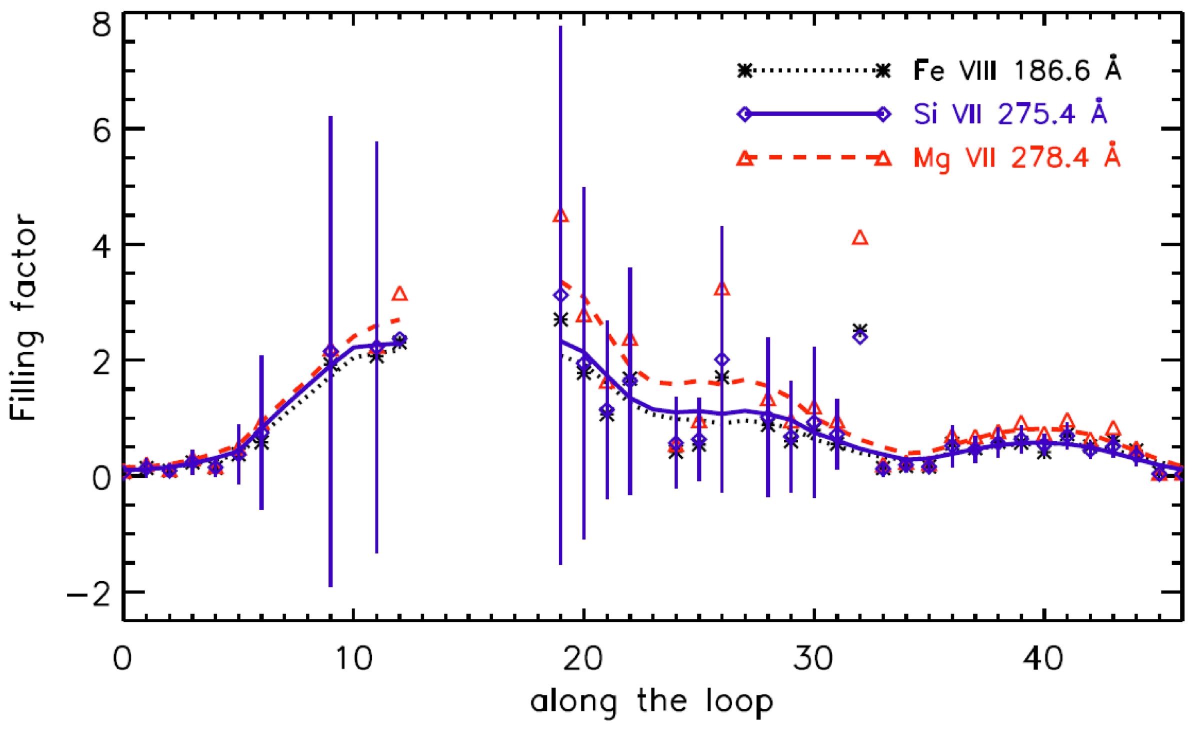

Figure 7. Plasma filling factor (ϕ) along the coronal loop from footpoint A to B as measured in different spectral lines.

D) Comparison with hydrostatic equilibrium:

The electron density profile for a loop in hydrostatic equilibrium is given by

$$n_e(h) = n_e(0)\, exp\left(-\frac{h}{\lambda(T_e)}\right), \quad \text{where} \quad \lambda(T_e) = \frac{k_b T_e}{\mu m_H g} \approx 46\left[\frac{T_e}{1\,MK}\right][Mm],$$

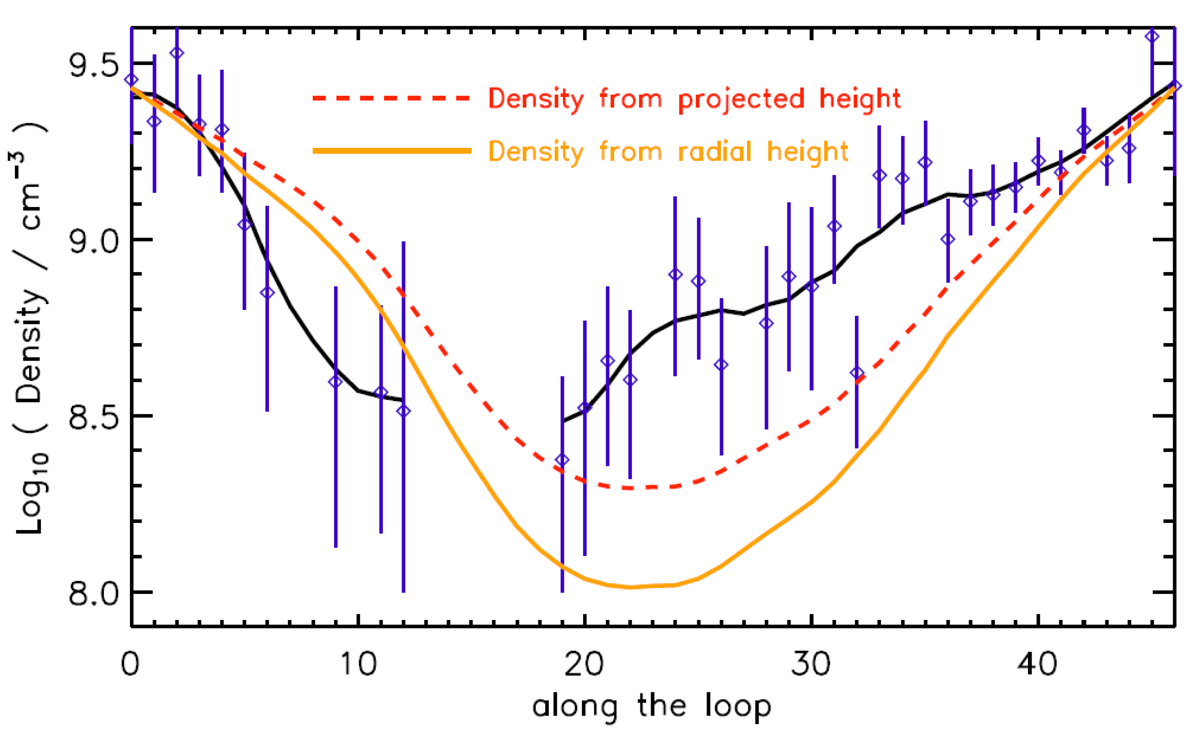

Figure 8. Comparison of density as measured using the Mg VII 280.75 and 278.39 Å line ratio (plotted with a diamond symbol) from footpoint A to B with the density expected from a hydrostatic model at temperature 0.73 MK obtained from projected (dashed line) and radial (dot–dashed line) heights of the loop.

Summary:

We found that the observed densities in the left segment of the loop were lower (i.e., underdense) than that expected from the isothermal hydrostatic model. However, it was higher (i.e., overdense) for the right segment of the loop (see Figure 8). This suggests a non-symmetric density profile along the loop. The results obtained here for the complete loop provide an opportunity for comparison with various loop models. The near isothermal nature of the loop along with the small filling factor and overdensity (super-hydrostatic) are in agreement with the impulsive heating model (Cargill & Klimchuk 2004; Klimchuk 2006). However, the observations presented here show the overdensity in only one part of the loop. Moreover, the quasi-steady footpoint heating model, which drives the thermal non-equilibrium solutions, may explain the observed properties of the loop studies here (e.g., Lionello et al. 2013; Mikić et al. 2013). Therefore, it will be interesting and important to measure physical properties such as densities, flows, and geometries of many well-observed coronal loops and compare their properties with various loop heating models to make generic conclusive statements on their heating and dynamics.

Reference: G.R. Gupta, D. Tripathi, H.E. Meson, 2015 ApJ, 800, 140